Discrete dislocation and continuum descriptions of plastic flow

Needleman, A.; van der Giessen, E.

Published in:
Materials science and engineering a-Structural materials properties microstructure and processing

DOI:
10.1016/S0921-5093(00)01684-1

Publication date:
2001

ELSEVIER

Materials Science and Engineering A309–310 (2001) 1–13

MATERIALS SCIENCE & ENGINEERING A

www.elsevier.com/locate/msea

Discrete dislocation and continuum descriptions of plastic flow

A. Needleman [a,*], E. Van der Giessen [b]

[a] *Division of Engineering, Brown University, Providence, RI 02912, USA*
[b] *Delft University of Technology, Koiter Institute Delft, Mekelweg 2, 2628 CD Delft, Netherlands*

Abstract

Conventional continuum mechanics models of inelastic deformation processes are size scale independent. In contrast, there is considerable experimental evidence that plastic flow in crystalline materials is size-dependent over length scales of the order of tens of microns and smaller. Geometrically necessary dislocations play a key role in this regard. At present there is no generally accepted framework for analyzing the size-dependent response of a plastically deforming crystal. Dislocation-based plasticity can provide information on the form of the governing equations and the boundary conditions, as well as material properties. Two model problems that highlight the limitations of conventional continuum plasticity are considered. For each problem, solutions using discrete dislocation plasticity and a recently proposed nonlocal continuum formulation are compared. The capabilities and limitations of the currently available nonlocal continuum theories are discussed.

Keywords: Continuum plasticity theory; Dislocation plasticity; Size effects

1. Introduction

In conventional continuum crystal plasticity, the plastic flow response is characterized by the slip system flow strengths and by their hardening. Boundary value problems are formulated using general conservation laws — mass, linear momentum and angular momentum — and requiring displacements and/or tractions (force/unit area) to be specified on the surface. Given the slip system geometry, descriptions of the flow strengths and the hardening matrix can be given on purely phenomenological grounds or on the basis of physical considerations of the underlying mechanisms. There is a large body of literature on such physically based dislocation models, e.g. [1]. Most of these focus on single slip and there are still challenges remaining, e.g. to develop such models for latent hardening. Indeed, three-dimensional dislocation dynamics has recently shown that it is potentially capable of filling in this gap [2,3].

Regardless of the details, conventional continuum plasticity theory predicts that the plastic response of crystalline solids is size-independent. In contrast, there is a considerable body of experimental evidence that this size independence breaks down at length scales of the order of tens of microns and smaller, e.g. [4–8]. Various phenomenological plasticity theories have been proposed that give rise to such size dependence, e.g. [9–17]. The structure of these theories varies to the extent that what properties characterize the material and what information is needed to pose boundary value problems depends on the theoretical framework used. Although dislocation-based arguments are used as motivation, these theories are phenomenological. The various forms are not quantitatively derived from considerations of the behavior of dislocations. An overview of mesoscale plasticity modeling with a focus on computational issues is given in [18].

For size-dependent plasticity, there is a need for dislocation-based plasticity theory to provide information on the form of the governing equations and the boundary conditions, as well as to provide material properties. A statistical mechanics of discrete dislocations needs to be developed to derive the size-dependent mechanical response of a plastically deforming crystal; an initial step in this direction for single slip has been taken by Groma and Balogh [19]. However, a complete theory is not available. What is available is a method for solving discrete dislocation plasticity boundary value problems, the solutions of which can then be compared with the predictions of various size-dependent phenomenological continuum plasticity theories. Here, two such comparisons are discussed.

To begin, conventional continuum plasticity is discussed with an emphasis on the assumptions underlying the formulation. A framework, Van der Giessen and Needleman [20], for solving boundary value problems where plastic flow arises from the collective motion of dislocations is briefly

* Corresponding author. Tel.: +1-401-863-2863; fax: +1-401-863-1157.
E-mail address: needle@engin.brown.edu (A. Needleman).

0921-5093/01/$ – see front matter
PII: S0921-5093(00)01684-1

reviewed and solutions to two model problems that highlight the limitations of conventional continuum plasticity are presented. The nonlocal crystal plasticity theories of Shu and Fleck [13] and of Acharya and Bassani [14] are presented and their predictions compared with the corresponding discrete dislocation solutions.

2. Conventional continuum plasticity

We consider a continuous body, a collection of material points occupying some region of space, in a chosen reference configuration. The position of a material point in the reference configuration, relative to a fixed Cartesian frame, is denoted by x_i.[1] In the current configuration, the material point at x_i in the reference configuration is at $\bar{x}_i$. The Cartesian components of the displacement field are defined by

$$u_i(x_k, t) = \bar{x}_i(x_k, t) - x_i \tag{1}$$

Here, time, t, is a parameter that orders a sequence of equilibrium states.

Conventional continuum mechanics is local in that the mechanical response at a point x_k only depends on the displacement through its gradient at that point. With attention restricted to small deformations, the strain tensor ϵ_{ij} and the rotation tensor ω_{ij} are introduced as the symmetric and anti-symmetric parts of $\partial u_i(x_k, t)/\partial x_j$ via

$$\frac{\partial u_i}{\partial x_j} = \epsilon_{ij} + \omega_{ij} \tag{2}$$

with

$$\epsilon_{ij} = \frac{1}{2}\left(\frac{\partial u_i}{\partial x_j} + \frac{\partial u_j}{\partial x_i}\right), \qquad \omega_{ij} = \frac{1}{2}\left(\frac{\partial u_i}{\partial x_j} - \frac{\partial u_j}{\partial x_i}\right) \tag{3}$$

Also, continuum theory relies on the notion of compatibility. This is the requirement that the strain and rotation fields are derivable from a single-valued function $u_i(x_k)$. Thus, given a closed curve C in the body

$$\oint_C [\epsilon_{ij} + \omega_{ij}]\, \mathrm{d}x_j = \oint_C \frac{\partial u_i}{\partial x_j}\, \mathrm{d}x_j = 0 \tag{4}$$

because the two end points are the same physical point and the displacement is single-valued and continuously differentiable.

In conventional continuum mechanics it is assumed that material elements only transmit forces. The traction vector, the force per unit area, acting on a surface with normal n_i is given by

$$T_i = \sigma_{ij} n_j \tag{5}$$

where σ_{ij} are the components of the stress tensor.

[1] Cartesian tensor notation is employed with repeated lower case Latin subscripts implying a summation from 1 to 3.

The balance of linear momentum, neglecting inertia effects and body forces, takes the form

$$\frac{\partial \sigma_{ij}}{\partial x_j} = 0 \tag{6}$$

and the balance of angular momentum is expressed by

$$\sigma_{ij} = \sigma_{ji} \tag{7}$$

The governing equations are completed by a set of constitutive equations. The simplest example being Hooke's law for which

$$\sigma_{ij} = L_{ijkl}\epsilon_{kl} \tag{8}$$

where L_{ijkl} is the tensor of elastic moduli. Substituting (8) into (6), and using the symmetry of the stress and strain tensors, gives the governing partial differential equations of elasticity theory

$$\frac{\partial}{\partial x_j}\left(L_{ijkl}\frac{\partial u_k}{\partial x_l}\right) = 0 \tag{9}$$

Eq. (9) together with appropriate boundary conditions give rise to a well-posed problem that can be solved analytically or numerically. The simplest boundary conditions are that

$$u_i = U_i^0(x_k) \quad \text{on part of the surface} \tag{10}$$

$$T_i = T_i^0(x_k) \quad \text{on the complementary part of the surface} \tag{11}$$

where u_i^0 and T_i^0 are the prescribed displacement and traction, respectively.

Eqs. (3), (6) and (7) express the geometry of deformation and basic balance laws whereas the constitutive relation, e.g. (9), purports to say something about the behavior of a class of materials that must be determined from some lower level theory or from experiment.

Conventional continuum plasticity, as it pertains to crystalline metals, provides a phenomenological description of deformation due to dislocation motion. Because plastic flow is history-dependent, the stress cannot, in general, be written as a direct function of strain. The role of the constitutive relation now is, given the current state of the material, to relate the stress rate to the strain rate. At each instant of time, the strain rate is written as the sum of an elastic part and a plastic part

$$\dot{\epsilon}_{ij} = \dot{\epsilon}_{ij}^{\mathrm{e}} + \dot{\epsilon}_{ij}^{\mathrm{p}} \tag{12}$$

Here, and subsequently, a superposed dot denotes differentiation with respect to time. From (8), the elastic part is obtained as

$$\dot{\epsilon}_{ij}^{\mathrm{e}} = L_{ijkl}^{-1}\dot{\sigma}_{kl} \tag{13}$$

while $\dot{\epsilon}_{ij}^{\mathrm{p}}$ is obtained from a plastic flow rule.

For single crystals, with plastic flow occurring by simple shear on a specified set of slip planes, the plastic strain rate is given by

$$\dot{\epsilon}^{\mathrm{p}}_{ij} = \sum_{\alpha} \frac{1}{2} \dot{\gamma}^{(\alpha)} (s^{(\alpha)}_i m^{(\alpha)}_j + s^{(\alpha)}_j m^{(\alpha)}_i) \tag{14}$$

where $s^{(\alpha)}_i$ specifies the slip direction for slip system α and $m^{(\alpha)}_i$ the slip plane normal for slip system α.

Now each slip system has a flow strength, say $\bar{\tau}^{(\alpha)}$, that evolves according to

$$\dot{\bar{\tau}}^{(\alpha)} = \sum_{\beta} h_{\alpha\beta} \dot{\gamma}^{(\beta)} \tag{15}$$

The plastic properties are the initial flow strength of each system and the hardening matrix $h_{\alpha\beta}$.

The deformation history is determined by solving a sequence of rate boundary value problems of the form

$$\frac{\partial}{\partial x_j} \left(L_{ijkl} \frac{\partial \dot{u}_k}{\partial x_l} \right) - \frac{\partial}{\partial x_j} (L_{ijkl} \dot{\epsilon}^{\mathrm{p}}_{kl}) = 0 \tag{16}$$

with rate boundary conditions

$$\dot{u}_i = \dot{U}^0_i(x_k) \quad \text{on part of the surface} \tag{17}$$

$$\dot{T}_i = \dot{T}^0_i(x_k) \quad \text{on the complementary part of the surface} \tag{18}$$

Once the plastic properties are known, the system of equations (16)–(18) can be used to determine the plastic response of a system or structure to some given loading history. There is a rich literature concerned with calculating the flow strength and hardening of crystalline solids from the underlying mechanisms of plastic flow. In particular, discrete dislocation plasticity has been used to calculate the flow strength and hardening of metal crystals, e.g. [2,3].

An immediate conclusion from (16)–(18) is that the mechanical response depends only on ratios of geometric length and not on absolute size. In contradiction to this, there is a considerable body of experimental evidence that plastic flow processes in crystalline solids are inherently size-dependent over a scale that ranges from a fraction of a micron to a hundred microns or so [4–8]. When the size dependence of plastic flow is accounted for in terms of a phenomenological nonlocal theory, the plastic flow response is no longer necessarily described by (16)–(18).

3. Discrete dislocation plasticity

Plastic flow in crystalline metals mainly arises from the collective motion of large numbers of dislocations. Although dislocations are atomic scale defects, their elastic interactions can be modeled by considering them as line singularities in an elastic solid. A framework for solving boundary value problems where plastic flow is represented by the collective motion of dislocations so modeled was developed by Van der Giessen and Needleman [20]. The key point [20,21] is that the stresses and strains are written as superpositions of fields due to the discrete dislocations, which are singular inside the body, and image fields that enforce the boundary conditions and any continuity conditions across internal phase boundaries. This leads to a linear elastic boundary value problem for the smooth image fields that can be solved by standard numerical techniques.

In general, the computation of the deformation history is carried out in an incremental manner with each time step involving three main computational stages: (i) determining the Peach–Koehler forces on the dislocations; (ii) determining the rate of change of the dislocation structure caused by the motion of dislocations, the generation of new dislocations, their mutual annihilation, and their possible pinning at obstacles; (iii) determining the stress and strain state for the updated dislocation arrangement.

In the current state, (9) is satisfied along with appropriate boundary conditions of the form (10) and (11). Superposition is used to write the displacement, strain and stress fields as

$$u_i = \tilde{u}_i + \hat{u}_i, \qquad \epsilon_{ij} = \tilde{\epsilon}_{ij} + \hat{\epsilon}_{ij}, \qquad \sigma_{ij} = \tilde{\sigma}_{ij} + \hat{\sigma}_{ij} \tag{19}$$

The $(\tilde{\ })$ fields are the sum of the fields of the individual dislocations, in their current configuration, and give rise to tractions $\tilde{T}_i$ and displacements $\tilde{U}_i$ on the boundary of the body.

The $(\hat{\ })$ fields represent the image fields that correct for the actual boundary conditions on the boundary. The $(\tilde{\ })$ fields satisfy (9) identically and the governing equations for the $(\hat{\ })$ fields in a single-phase material are

$$\frac{\partial \hat{\sigma}_{ij}}{\partial x_j} = 0, \qquad \hat{\epsilon}_{ij} = \frac{1}{2} \left(\frac{\partial \hat{u}_i}{\partial x_j} + \frac{\partial \hat{u}_j}{\partial x_i} \right), \quad \hat{\sigma}_{ij} = L_{ijkl} \hat{\epsilon}_{kl} \tag{20}$$

From (10) and (11), the boundary conditions for the $(\hat{\ })$ fields are

$$\hat{\sigma}_{ij} n_j = T^0_i - \tilde{T}_i \tag{21}$$

on that part of the surface where tractions are prescribed and

$$\hat{u}_i = U^0_i - \tilde{U}_i \tag{22}$$

on that part of the surface where displacements are prescribed. Here, T^0_i and U^0_i are the prescribed tractions and displacements, respectively.

The long-range interactions between dislocations are accounted for through the continuum elasticity fields. Short-range dislocation interactions are incorporated into the formulation through a set of constitutive rules. These include relations for dislocation nucleation, annihilation, dislocation intersections, cross-slip and for the kinetics of dislocation motion (see, e.g., [22]). The thermodynamic driving force for these mechanisms is the Peach–Koehler force. This force represents the fact that when dislocation I glides an amount $\delta s^{(I)}$ in its slip plane, there is a

contribution to the internal virtual work of magnitude

$$\sum_I \int_{\mathcal{L}^{(I)}} f^{(I)} \delta s^{(I)} \, \mathrm{d}\ell \tag{23}$$

where $\mathcal{L}^{(I)}$ is the Ith dislocation line. This force $f^{(I)}$ is the glide component of the Peach–Koehler force, and can be calculated as

$$f^{(I)} = b_i^{(I)} \left(\hat{\sigma}_{ij} + \sum_{J \neq I} \tilde{\sigma}_{ij}^{(J)} \right) m_j^{(I)} \tag{24}$$

where m_j is the slip plane normal.

Annihilation of two dislocation segments on the same slip plane with opposite signed Burgers vector occurs when they are within a material-dependent, critical annihilation distance. In the calculations to date, the magnitude of the glide velocity $v^{(I)}$ has been taken to be linearly related to the Peach–Koehler force magnitude through the linear drag relation

$$f^{(I)} = B v^{(I)} \tag{25}$$

where B is the drag coefficient.

The calculations to be discussed subsequently were carried out in a two-dimensional plane strain framework where all the dislocations are edge dislocations. However, the theoretical formulation is fully three-dimensional and three-dimensional calculations are beginning to be carried out [23].

In this framework, both the dislocation patterns that form and the stress–strain response emerge as outcomes of the solution to a boundary value problem. Furthermore, there is a material parameter with the dimensions of length — the Burgers vector magnitude. As a consequence, the response predicted by discrete dislocation plasticity can be size-dependent. The geometrically necessary dislocations of Nye [24] and Ashby [25] play a key role in this regard.

The density of geometrically necessary dislocations can be determined by a straightforward geometric argument due to Nye [24]. Consider a plane crossed by dislocations with Burgers vector $b_i^{(I)}$ and with $t_i^{(I)}$ the tangent to the dislocation line. Suppose $N^{(I)}$ of these dislocations of type I cross a unit area normal to $t_i^{(I)}$. Then, the number crossing a unit area with normal v_j is $N^{(I)} v_j t_j^{(I)}$. The net Burgers vector is $B_i^{(I)} = N^{(I)} v_j t_j^{(I)} b_i^{(I)}$, which gives a measure of the net dislocation density for dislocations of this type. The total net dislocation density is obtained by summing the contributions of all dislocation types to give

$$B_i = v_j \sum_I N^{(I)} t_j^{(I)} b_i^{(I)} \tag{26}$$

Since in a purely stochastic distribution, there are as many dislocations having Burgers vector $b_i^{(I)}$ as $-b_i^{(I)}$, the net Burgers vector vanishes for such a distribution. Thus, B_i gives a measure of the density of geometrically necessary dislocations. In the following, we consider two idealized problems that highlight effects of geometrically necessary dislocations.

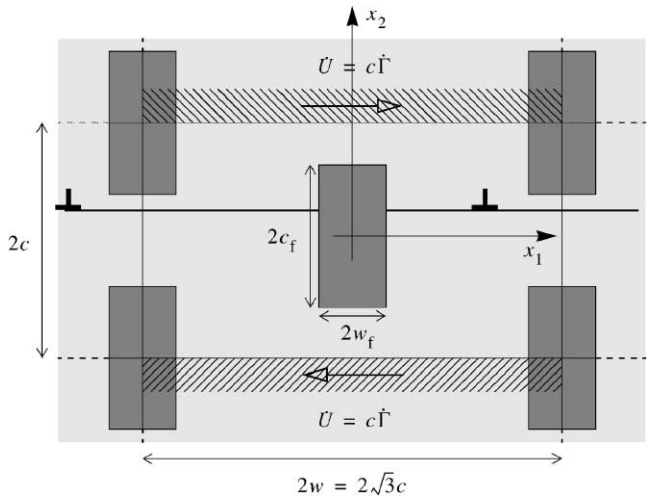

Fig. 1. Unit cell of a composite material with a doubly periodic array of elastic particles. All slip planes are taken to be parallel to the applied shear direction (x_1).

3.1. Model metal–matrix composite

The first problem considered is the deformation of a two-dimensional model material containing rectangular particles arranged in a hexagonal packing as illustrated in Fig. 1. In [26,27], the cell is subjected to plane strain, simple shear, which is prescribed through the boundary conditions

$$u_1 = \pm c\Gamma, \qquad u_2 = 0 \quad \text{along } x_2 = \pm c \tag{27}$$

where Γ is the applied shear. Periodic boundary conditions are imposed along the lateral sides $x_1 = \pm w$. Edge dislocations, all having the same Burgers vector magnitude, b, were considered on a single slip system with the slip plane normal m_i in the x_2-direction and with the glide direction s_i in the x_1-direction.

Two reinforcement morphologies were analyzed having the same area fraction but different geometric arrangements of the reinforcing phase. In one morphology, material (i), the particles are square and are separated by unreinforced veins of matrix material while in the other, material (iii), the particles are rectangular and do not leave any unreinforced veins of matrix material. The matrix was taken to be free of mobile dislocations initially, but to have a specified density of obstacles possibly representing forest dislocations. As the shear strain increases, dislocation dipoles are generated using a two-dimensional model of Frank–Read sources, dislocations move and possibly get pinned at obstacles or at the matrix–particle interface.

Fig. 2 shows composite stress–strain curves for these two morphologies, while Fig. 3 gives examples of the dislocation distributions predicted by the calculations. The shear-stress–shear-strain response of material (i) has a peak

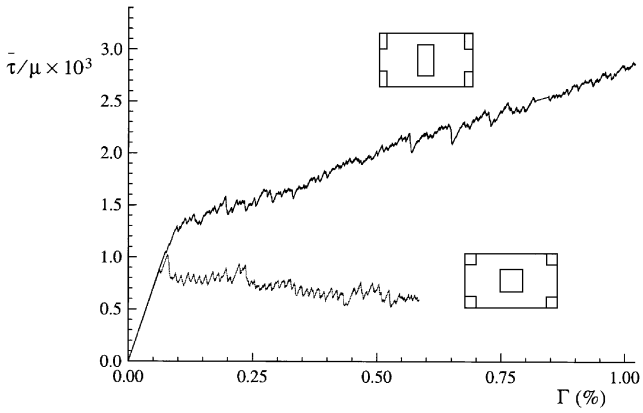

Fig. 2. Shear stress versus shear strain for two reinforcement morphologies. The case that exhibits nearly linear hardening is termed material (iii) and the other case is termed material (i). Results from [26].

stress followed by a slight softening, whereas material (iii) exhibits more or less linear hardening. Since, for material (i) the motion of dislocations in a vein is not blocked by the reinforcement, there is a progressive concentration of all dislocation activity into one of the veins in the cell at rather small strains. On the other hand, for the reinforcement morphology termed material (iii), the central reinforcement must rotate to accommodate the shear, leading to a strong piling-up of dislocations against the reinforcement sides (Fig. 3). These are the geometrically necessary dislocations of Ashby [25].

Fig. 4 shows the shear stress versus shear strain responses for initially dislocation-free materials with three size scales of particles, specified by $h/L = 0.5$, 1 and 2, where L is defined as $L = 4000b$ and, as the inset shows, h is the same as c in Fig. 1. The random distributions of dislocation sources and obstacles for each of the three materials were such that the corresponding densities were roughly the same. The calculations show a systematic trend that the composite hardening increases with decreasing particle size. This was confirmed by computations using different distributions of sources and obstacles, and by simulations for intermediate particle sizes. On the other hand, for the composite morphology denoted as material (i) no size effect was found [27].

The key features of the results for a continuum theory of plasticity are (i) the inferred matrix stress–strain response depends on the reinforcement morphology as well as on the reinforcement volume fraction, (ii) there is a size

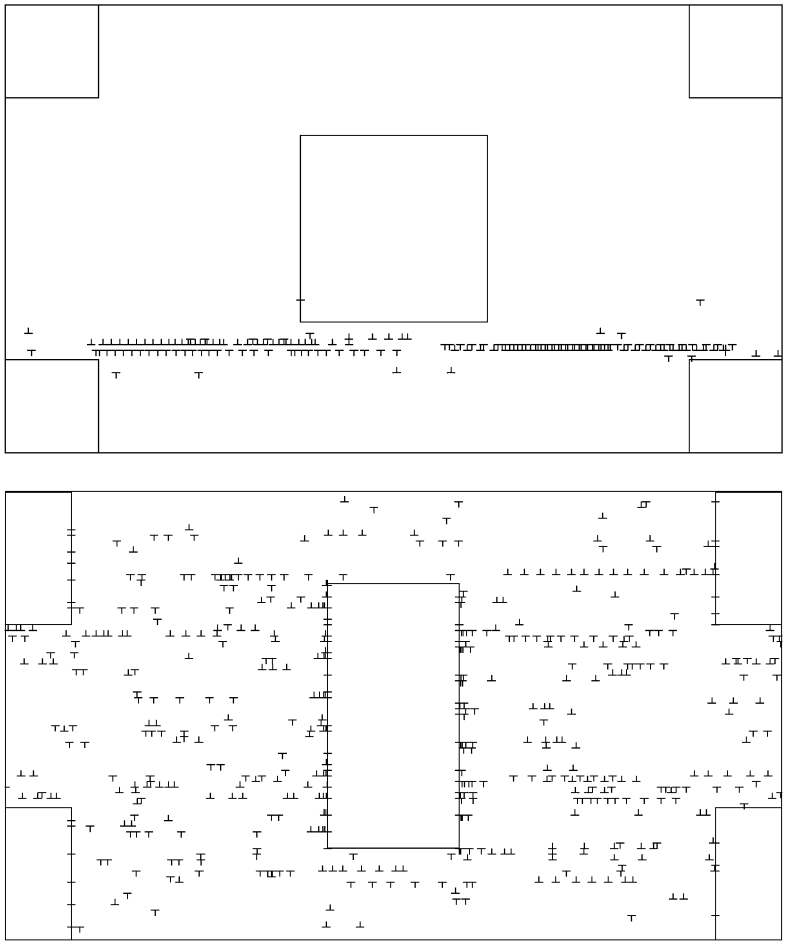

Fig. 3. Dislocation structures for material (i) (top) and material (iii) (bottom). From [26].

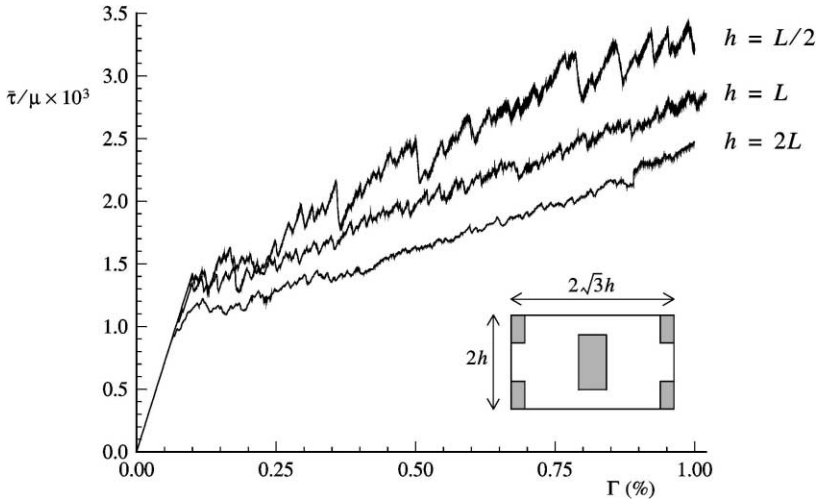

Fig. 4. Shear stress versus shear strain for various size scales of reinforcement. Results from [27].

dependence for morphologies where deformation requires geometrically necessary dislocations, and (iii) this size dependence is mainly seen in the hardening. Solutions based on the classical continuum plasticity framework described in Section 2 cannot exhibit these features.

3.2. Shear of a constrained layer

Shu et al. [28] analyzed simple shear of a crystalline layer. As sketched in Fig. 5 the layer is of height H in the x_2-direction with shearing along the x_1-direction. Plane strain is assumed and the layer is unbounded in the x_1- and x_3-directions. All field quantities are taken to be periodic in x_1 with period w (see Fig. 5). The boundary conditions are

$$\begin{aligned} &u_1 = 0, \quad u_2 = 0 \quad \text{along } x_2 = 0, \\ &u_1 = H\Gamma, \quad u_2 = 0 \quad \text{along } x_2 = H \end{aligned} \tag{28}$$

where Γ is the prescribed shear. A single phase material is considered and there are two slip systems which are oblique to the shearing direction. Length scales in this problem include the Burgers vector b, the layer height H, the spacing between active slip planes, d, and the linear spacing of sources on each slip plane, d_{nuc}. The discrete dislocation results depend on three non-dimensional lengths, e.g. d/b, d/H and d_{nuc}/d.

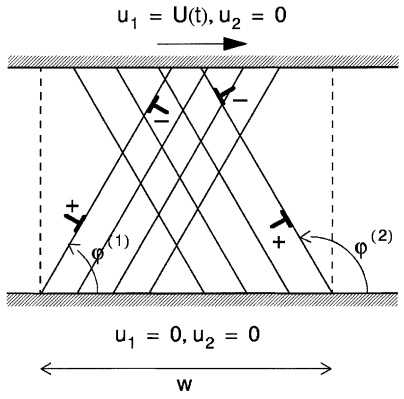

Fig. 5. Illustration of the problem formulation and boundary conditions for simple shear with two active slip systems.

Crystals oriented for both single slip and symmetric double slip were analyzed. Strain profiles across the crystal computed on the basis of discrete dislocation plasticity are shown in Fig. 6. Here, the average shear strain is defined as

$$\gamma(x_2) = \frac{\mathrm{d}u_1^{\text{ave}}}{\mathrm{d}x_2}, \quad u_1^{\text{ave}}(x_2) = \frac{1}{w}\int_0^w u_1(x_1, x_2)\,\mathrm{d}x_1 \tag{29}$$

The jagged curves show the calculated average shear strain profiles, while the smooth curves are an exponential fit used to facilitate identification of the boundary layer width. The boundary layer in double slip is quite pronounced with the local shear strain $\gamma(x_2)$ approaching values close to zero at both edges $x_2 = 0$ and H.

Fig. 7 shows stress–strain curves under double slip for layers having various heights. The material properties are kept fixed. Each of the hardening responses is linear on an average and is fit by a straight line. The dots indicate the initial back-extrapolated flow strengths, τ_{F}. The tangent modulus reduces gradually as the crystal height becomes smaller, although the values for the largest crystals do not order. The back-extrapolated initial flow strengths, however, do exhibit a clear size effect with the smallest crystal having the highest yield strength. In fact, the values of τ_{F} were found to scale almost linearly with $(d/H)^{1/2}$. Blocked slip at the upper and lower boundaries of the layer gives rise to the gradient of the average strain and to the size effect.

The boundary layer in single slip was found to be much less pronounced. Also, the dislocation distributions in single slip gave rise to a very large back stress, so that in single slip, there is enormous hardening after initial yield. Because of this back stress, the overall shear stress versus shear strain relation in single slip was insensitive to model details.

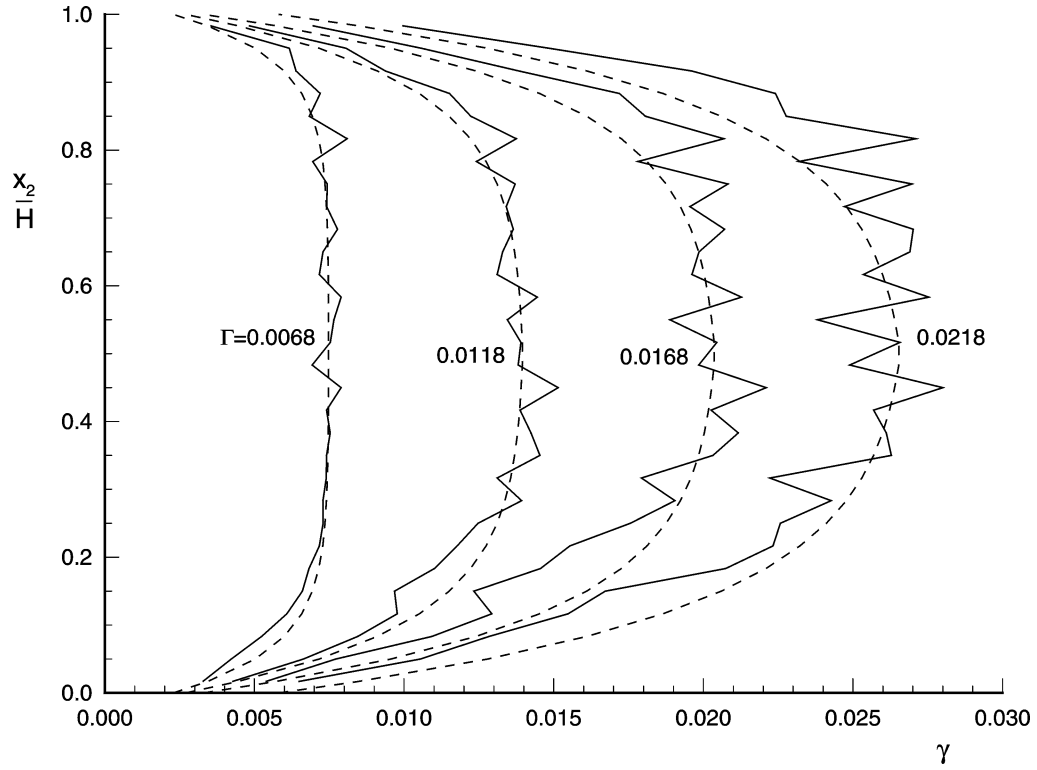

Fig. 6. Shear strain profiles at various values of the applied shear Γ for double slip with $H = 1\,\mu$m. The dashed lines are fitted exponential strain profiles. From [28].

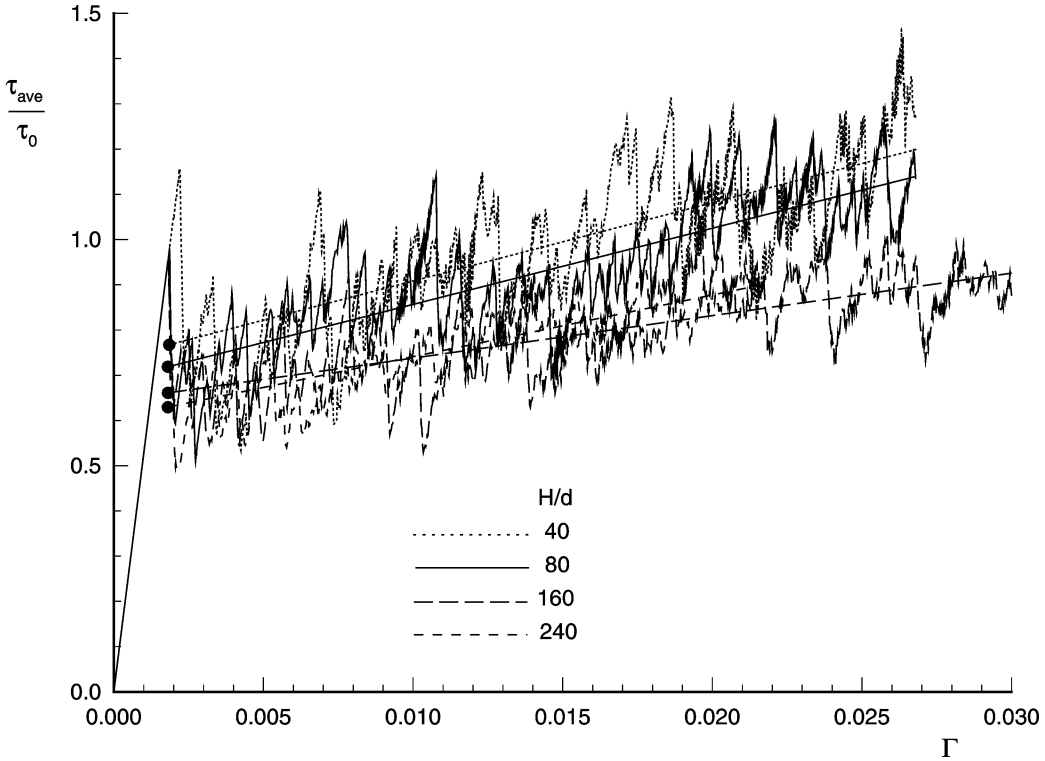

Fig. 7. Average shear stress response to applied macroscopic shear Γ during double slip for various layer thicknesses H/d. From [28].

It should be noted that a solution in which γ is independent of x_2 is possible and, in fact, Shu et al. [28] did not find a boundary layer when a sufficiently high Peierls barrier to glide was introduced. Thus, the discrete dislocation results show that a boundary layer is possible in this simple shear problem, but its occurrence and extent depend on the material properties and on the slip geometry. The existence of a strain gradient implies the presence of geometrically necessary dislocations in the sense of Ashby [25], although in this case these dislocations are not solely induced by the geometry of deformation. Evidence for the existence of such geometrically necessary dislocations at the interface in an aluminum bicrystal is presented in [29].

The discrete dislocation analyses indicate that (i) back stress effects are much less for crystals in the symmetric double slip configuration than for single slip, (ii) in symmetric double slip a clear size effect is found for the initial flow strength, but not for the hardening, and (iii) the boundary layers thicken with increasing strain. These boundary layer and size effects do not occur within the framework of conventional plasticity theory.

4. Nonlocal continuum plasticity

Representative values for dislocation densities in deformed crystalline metals are in the range 10^{13}–$10^{15}\,\mathrm{m}^{-2}$. To carry out a discrete dislocation calculation for a $100\,\mu\mathrm{m}^3$ cube for a dislocation density of $10^{13}\,\mathrm{m}^{-2}$ would require dealing with of the order of 10^8 dislocation segments (assuming a segment length of $0.1\,\mu\mathrm{m}$). Computational considerations will limit the scope of direct discrete dislocation plasticity calculations for the foreseeable future.

Hence, there is a clear need for a phenomenological theory of size-dependent plastic flow. To incorporate such size dependence in a phenomenological continuum theory, the stress at a point no longer just depends on the displacement through its gradient at that point. One type of nonlocal theory involves the mechanical response depending on higher displacement gradients, i.e. gradients of strain and, possibly, rotation.

A nonlocal crystal plasticity theory is needed to make a clear connection with discrete dislocation plasticity. However, much of the development in nonlocal continuum plasticity has taken place within the context of isotropic hardening. The usual rationale for using an isotropic theory of plasticity is that the theory pertains to polycrystals and the response is averaged over many crystal orientations. At the scale where gradient effects come into play, relevant length scales are of the order of the crystal size (or smaller) so that the effect of the discreteness of slip systems is not negligible. Several nonlocal crystal plasticity theories are now available and predictions of those of Shu and Fleck [13] and of Acharya and Bassani [14] have been compared with corresponding predictions of discrete dislocation plasticity.

Although each of these theories is based on the intimate connection between the density of geometrically necessary dislocations and plastic strain gradients, they lead to different boundary value formulations. Writing the displacement gradient as the sum of an elastic part, u^{e}_{ij}, and a plastic part, u^{p}_{ij},

$$\frac{\partial u_i}{\partial x_j} = u^{\mathrm{e}}_{ij} + u^{\mathrm{p}}_{ij} \tag{30}$$

compatibility requires (4) to be satisfied by the total displacement gradient, but there is no basis for requiring u^{e}_{ij} or u^{p}_{ij} to be compatible. Instead, a contour integral of the plastic part can be used to define the net Burgers vector B_i by

$$B_i = \oint_C u^{\mathrm{p}}_{ij}\,\mathrm{d}x_j \tag{31}$$

Using Stokes' theorem,

$$B_i = \oint_C u^{\mathrm{p}}_{ij}\,\mathrm{d}x_j = \oint_S e_{jkl}\frac{\partial u^{\mathrm{p}}_{il}}{\partial x_k}\nu_j\,\mathrm{d}S = \oint_S \alpha_{ij}\nu_j\,\mathrm{d}S \tag{32}$$

where α_{ij} is Nye's dislocation density tensor, e_{ljk} the alternating tensor, ν_i the unit normal to a surface S whose boundary is the curve C. From (4) and (30), if u^{e}_{ij} is substituted for u^{p}_{ij}, the value of B_i only changes sign. The value of α_{ij} is related to the density of geometrically necessary dislocations within a crystal by (26).

Following Fleck et al. [4], the connection between geometrically necessary dislocations and slip gradients is seen by substituting (14) (together with the corresponding expression for the plastic rotation) into (32) to obtain

$$\alpha_{ij} = \sum_\alpha e_{jkl}\frac{\partial \gamma^{(\alpha)}}{\partial x_k}s^{(\alpha)}_i m^{(\alpha)}_l \tag{33}$$

It can be shown that α_{ij} only involves derivatives of $\gamma^{(\alpha)}$ in the slip plane (see [4]).

Acharya and Bassani [14] take the hardening to depend on the incompatibility measure α_{ij}, while Shu and Fleck [13] take the flow strength to be a function of α_{ij}. The structure that boundary value problems take is sensitive to this choice.

The proposal of Acharya and Bassani [14] is to write the hardening matrix in (15) as

$$h_{\alpha\beta} = h_{\alpha\beta}(\gamma^{(\kappa)}, \alpha_{ij}) \tag{34}$$

where α_{ij} is expressed in terms of the slip gradient by (33). A method for calculating the slip gradients appearing in (34) is needed but otherwise the theory of Acharya and Bassani [14] leads to a boundary value problem of the form (16)–(18) just as for conventional, size-independent plasticity.

On the other hand, when the strength is taken to be a function of α_{ij}, the structure of the boundary value problem changes and, as a consequence, additional boundary conditions need to be prescribed. In the nonlocal crystal plasticity theory of Shu and Fleck [13], formulated within the framework of Fleck and Hutchinson [12], the strain and the strain

gradients are written as the sum of elastic and plastic parts. The strain gradient tensor η_{ijk} is given by

$$\eta_{ijk} = \frac{\partial^2 u_k}{\partial x_i \partial x_j} \tag{35}$$

The plastic work rate per unit volume is given by

$$\begin{aligned}\dot{W}^{\mathrm{p}} &= \sigma_{ij}\dot{\epsilon}^{\mathrm{p}}_{ij} + \tau_{ijk}\dot{\eta}^{\mathrm{p}}_{ijk} \\ &= \sum_{\alpha}[\tau^{(\alpha)}\dot{\gamma}^{(\alpha)} + Q_S^{(\alpha)}\dot{\gamma}_S^{(\alpha)} + Q_M^{(\alpha)}\dot{\gamma}_M^{(\alpha)}] \\ &= \sum_{\alpha} s^{(\alpha)}\dot{\gamma}^{(\alpha)}\end{aligned} \tag{36}$$

where τ_{ijk} are the double stresses and

$$\begin{aligned}&\tau^{(\alpha)} = \sigma_{ij}s_i^{(\alpha)}m_j^{(\alpha)}, \\ &Q_S^{(\alpha)} = \tau_{ijk}s_i^{(\alpha)}m_j^{(\alpha)}s_k^{(\alpha)}, \quad Q_M^{(\alpha)} = \tau_{ijk}s_i^{(\alpha)}m_j^{(\alpha)}m_k^{(\alpha)}\end{aligned} \tag{37}$$

Since geometrically necessary dislocations are associated with slip gradients along the slip plane, gradient hardening is expected to enter only through $\dot{\gamma}_S^{(\alpha)}$. However, in this regard, it should be noted that $\dot{\gamma}_S^{(\alpha)}$ and $\dot{\gamma}_M^{(\alpha)}$ are independent kinematic quantities and are not equal to the spatial gradient of the slip rate $\dot{\gamma}^{(\alpha)}$. With attention restricted to hardening by geometrically necessary dislocations, the effective stress $s^{(\alpha)}$ and the effective strain rate $\dot{\gamma}^{(\alpha)}$ are given by

$$(s^{(\alpha)})^2 = (\tau^{(\alpha)})^2 + (\ell_S^{-1}Q_S^{(\alpha)})^2 \tag{38}$$

$$\dot{\gamma}_{\mathrm{e}}^{(\alpha)} = [(\dot{\gamma}^{(\alpha)})^2 + \ell_S^2(\dot{\gamma}_S^{(\alpha)})^2]^{1/2} \tag{39}$$

with

$$\dot{\gamma}^{(\alpha)} = \dot{\gamma}_{\mathrm{e}}^{(\alpha)}\frac{\tau^{(\alpha)}}{s^{(\alpha)}}, \qquad \dot{\gamma}_S^{(\alpha)} = \ell_S^{-2}\dot{\gamma}_{\mathrm{e}}^{(\alpha)}\frac{Q_S^{(\alpha)}}{s^{(\alpha)}} \tag{40}$$

The equilibrium equations take the form

$$\frac{\partial \sigma_{ji}}{\partial x_j} - \frac{\partial^2 \tau_{kji}}{\partial x_k \partial x_j} = 0 \tag{41}$$

with boundary conditions

$$\text{prescribe} \quad u_i \quad \text{or} \quad T_i \tag{42}$$

$$\text{prescribe} \quad n_j\frac{\partial u_i}{\partial x_j} \quad \text{or} \quad r_i = n_j n_k \tau_{kji} \tag{43}$$

where n_i is the surface normal, and

$$\begin{aligned}&T_i = n_k(\sigma_{ki} - \tau_{kji,j}) + n_k n_j \tau_{kji}(D_{\mathrm{p}}n_{\mathrm{p}}) - D_j(n_k\tau_{kji}), \\ &D_j = (\delta_{jk} - n_j n_k)\frac{\partial()}{\partial x_k}.\end{aligned} \tag{44}$$

In contrast with conventional continuum mechanics, material elements transmit higher-order tractions r_i as well as ordinary tractions T_i (now involving the double stress τ_{ijk} as well as the ordinary stress σ_{ij}). This is analogous to the situation in reduced dimensional theories of beams, plates and shells, where moments as well as tractions are transmitted across surfaces. As for these models, solutions to boundary value problems can be very sensitive to which higher-order boundary conditions are prescribed, as will be illustrated subsequently.

The constitutive description is completed by writing

$$\dot{\sigma}_{ij} = L_{ijkl}\dot{\epsilon}^{\mathrm{e}}_{ij} \tag{45}$$

$$\dot{\tau}_{ijm} = \ell_{\mathrm{e}}^2 L_{ijkl}\dot{\eta}^{\mathrm{e}}_{klm} \tag{46}$$

In this framework, the material parameters ℓ_S and ℓ_{e} are introduced. The length scale ℓ_S is associated with the effects of higher stresses on the flow strength and, presumably, evolves as the structure of geometrically dislocations develops. In addition, an elastic length scale ℓ_{e} needs to be specified.

The way that additional stress-type quantities and additional boundary conditions enter the crystal plasticity theory of Shu and Fleck [13] is not unique. For example, Gurtin [16] has developed a single crystal plasticity theory, that in the context of small strains and rotations, is based on writing the free energy, ψ, as

$$\psi = W(\epsilon^{\mathrm{e}}_{ij}) + \frac{1}{2}\tau_0\ell^2\left|\frac{\partial u^{\mathrm{p}}_{ij}}{\partial x_k}\right|^2 \tag{47}$$

where $W(\epsilon^{\mathrm{e}}_{ij})$ is the classical strain energy.

As a consequence of (47), the stress and therefore the resolved shear stress $\tau^{(\alpha)}$ is given by a nonlocal relation,

$$\begin{aligned}\tau^{(\alpha)} &= \bar{\tau}^{(\alpha)} - \tau_0\ell^2 s_i^{(\alpha)}m_j^{(\alpha)}\frac{\partial^2 u^{\mathrm{p}}_{ij}}{\partial x_k \partial x_k} \\ &= \bar{\tau}^{(\alpha)} - \tau_0\ell^2 s_i^{(\alpha)}m_j^{(\alpha)}\sum_{\beta}\frac{\partial^2 \gamma^{(\beta)}}{\partial x_k \partial x_k}s_i^{(\beta)}m_l^{(\beta)}\end{aligned} \tag{48}$$

where the evolution equation for $\bar{\tau}^{(\alpha)}$ is of the form (15). Moreover, there are the additional boundary conditions

$$\text{prescribe} \quad \dot{\gamma}^{(\alpha)} \quad \text{or} \quad \xi_i^{(\alpha)}n_i \tag{49}$$

where

$$\xi_i^{(\alpha)} = \tau_0\ell^2 m_k^{(\alpha)}s_l^{(\alpha)}\frac{\partial u^{\mathrm{p}}_{kl}}{\partial x_i} \tag{50}$$

The additional boundary conditions in this formulation are quite different from those in the theory of Shu and Fleck [13]. Also, as presented in [16], the theory involves the full gradient, not just the gradient terms associated with geometrically necessary dislocations.

4.1. Model metal–matrix composite

Bassani et al. [30] have carried out a comparison of the predictions of the nonlocal plasticity theory of Acharya and Bassani [14] with the discrete dislocation results of Cleveringa et al. [26,27] summarized in Section 3.1. For the model composite problem, there is only one non-vanishing

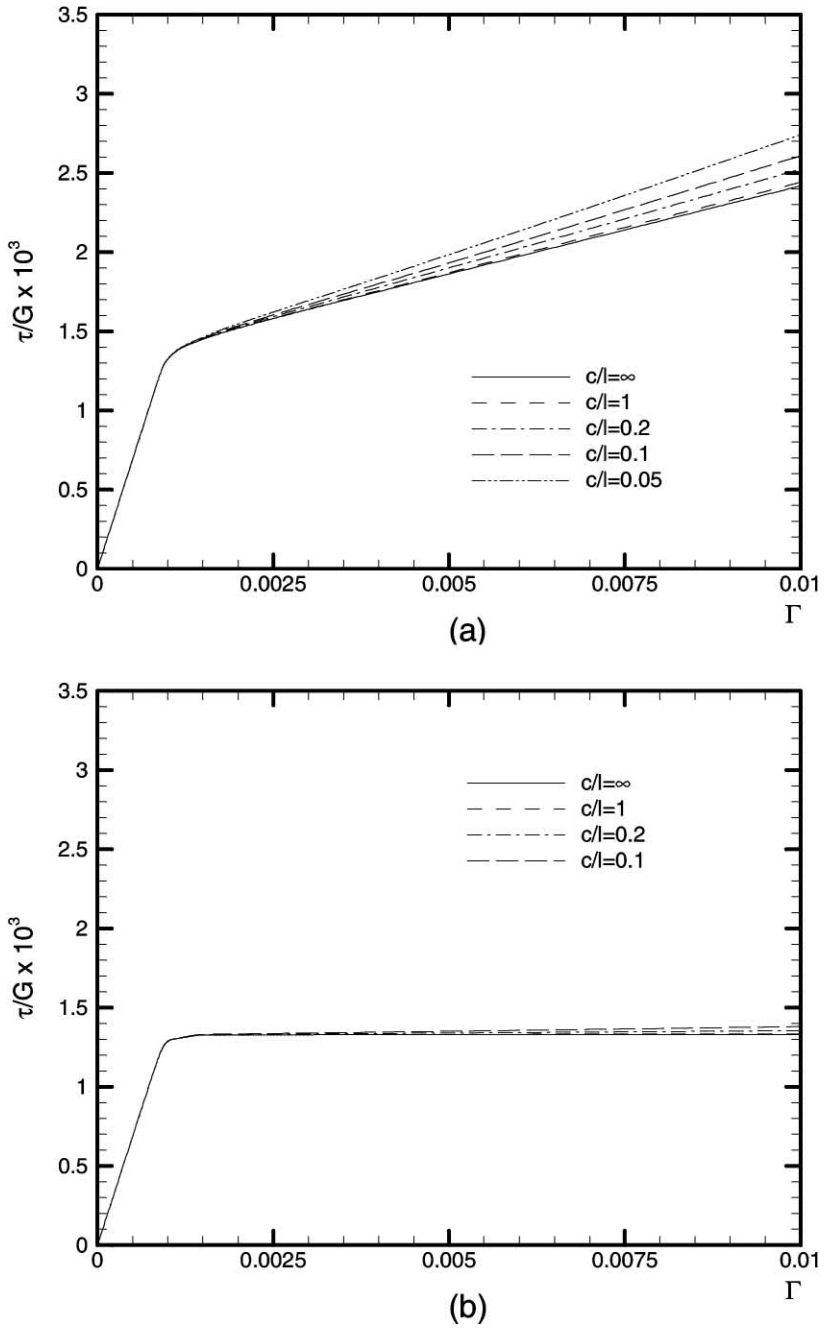

Fig. 8. Shear stress versus shear strain for two reinforcement morphologies using the nonlocal plasticity formulation of Acharya and Bassani [14]. (a) For material (iii). (b) For material (i). From [30].

component of α_{ij} which is equal to $\partial\gamma/\partial x_1$ (see Fig. 1). Bassani et al. [30] use a power law relation of the form

$$h\left(\gamma, \frac{\partial\gamma}{\partial x_1}\right) = h_0\left(\frac{\gamma}{\gamma_0} - 1\right)^{N-1}\left[1 + \ell^2\left(\frac{1}{\gamma_0}\frac{\partial\gamma}{\partial x_1}\right)^2\right]^p \quad (51)$$

where ℓ is the intrinsic length scale, and N and p are hardening parameters. It should be noted that, for multiple slip, how to apportion the effects of incompatibility among the various components of the hardening matrix for multiple slip is unresolved in the nonlocal theory of Acharya and Bassani [14].

Curves of the average shear stress τ_{ave} versus applied shear strain Γ are plotted in Figs. 8 and 9 for materials (i) and (iii), and for various cell sizes, c, normalized by the material length scale ℓ. Here, $c/\ell \to \infty$ corresponds to purely local behavior ($\ell = 0$). A reasonable set of matrix material parameters can be chosen in (34) that give rise to a response that is very similar to the behavior predicted by the discrete dislocation calculations for both material (i) and

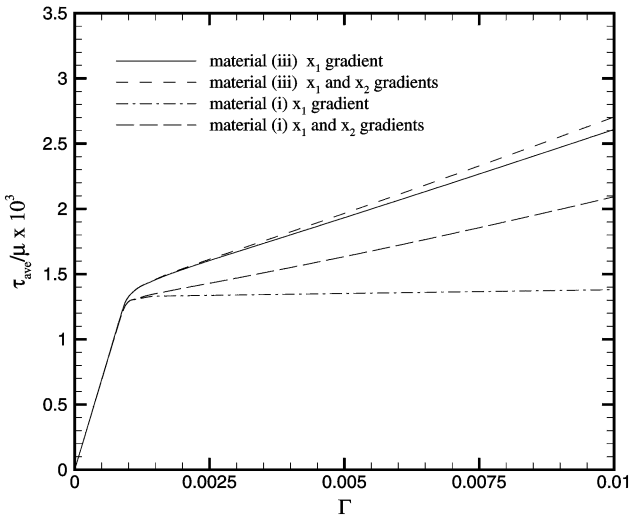

Fig. 9. Comparison of average shear stress τ_{ave} versus applied shear strain Γ for cases where the gradient hardening depends only on $\partial\gamma/\partial x_1$ with cases where the hardening depends on $\partial\gamma/\partial x_1$ and $\partial\gamma/\partial x_2$. From [30].

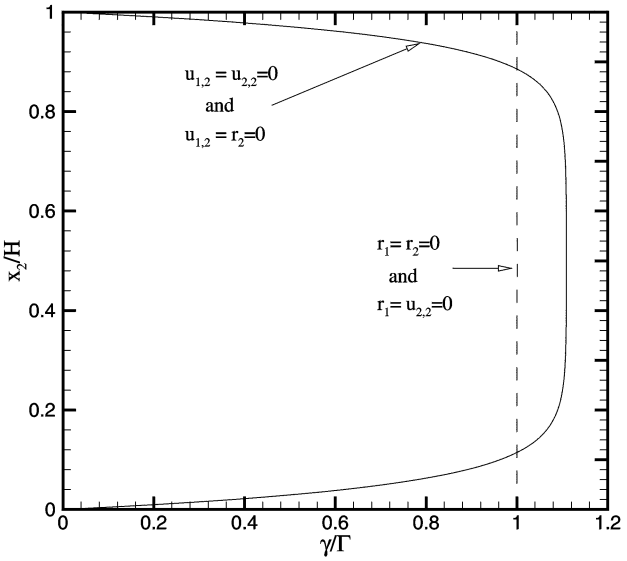

Fig. 10. Effect of choice of boundary conditions upon the shear traction τ_{ave} versus average shear strain Γ response by single-slip nonlocal theory, for $H/d = 2.3$ and $\ell = 10\ell_e = d$. From [28].

material (iii). For the nonlocal theory, the hardening is specified for one size and one morphology. The parameters characterizing the nonlocal behavior then predict a much greater size-dependent response for material (iii), where there are geometrically necessary dislocations, than for material (i), with smaller being harder.

For comparison, Bassani et al. [30] also considered the nonlocal response when the full gradient of slip, rather than the incompatibility measure, raises the level of hardening. Calculations were carried out where the term

$$\sqrt{\left(\frac{\partial\gamma}{\partial x_1}\right)^2+\left(\frac{\partial\gamma}{\partial x_2}\right)^2}$$

was used in (51) in place of $\partial\gamma/\partial x_1$. The effect of $\partial\gamma/\partial x_2$ was found to be significant for material (i) whereas it was small for material (iii), as seen in Fig. 10. The calculations with the gradient associated with geometrically necessary dislocations distinguish between the behaviors of material (i) and material (iii) whereas the calculations including the other slip gradient do not.

4.2. Shear of a constrained layer

For a homogeneous crystal, the solution to the boundary value problem (16) with the boundary conditions (28) corresponds to a state of uniform shear deformation. Thus, any local theory as well as the nonlocal theory of Acharya and Bassani [14] does not predict the existence of a boundary layer. On the other hand, with a nonlocal crystal theory of the type of Shu and Fleck [13] or Gurtin [16] which involve higher-order boundary conditions, there is the possibility that a boundary layer can emerge.

Shu et al. [28] analyzed simple shear using the nonlocal crystal theory of Shu and Fleck [13]. In addition to the boundary conditions (28), higher-order boundary conditions need to be imposed. These are

$$r_1 = \tau_{122} = 0 \quad \text{or} \quad u_{1,2} = 0 \tag{52}$$

$$r_2 = \tau_{222} = 0 \quad \text{or} \quad u_{2,2} = 0 \tag{53}$$

at $x_2 = 0$ and $x_2 = H$.

The effect of the choice of higher boundary condition is seen in Fig. 10 for single slip. Shu et al. [28] found a pronounced boundary layer using $u_{1,2} = u_{2,2} = 0$ or $u_{1,2} = r_2 = 0$. A switch in boundary condition from $u_{2,2} = 0$ to $r_2 = 0$ was found to have a small effect on the response. A stiffer stress–strain response was associated with the occurrence of the boundary layers; a somewhat more compliant response was associated with $r_1 = u_{2,2} = 0$ or $r_1 = r_2 = 0$.

The evolution of the boundary layers is shown in Fig. 11 for symmetric double slip using the boundary conditions $u_{1,2} = u_{2,2} = 0$. In symmetric double slip, the length parameter $\ell = \ell_S/\sin\phi$ is introduced, where ϕ gives the slip system orientation relative to the shear direction. The values $\ell = \ell_e = 0.1\,\mu\text{m}$ are used for the symmetric double slip calculations in Fig. 11, which captures the size effect and is consistent with the active slip band spacing found in the discrete dislocation calculations. However, this value of ℓ overestimates the thickness of the boundary layer in shear strain. It is noteworthy that a relatively large value for the elastic characteristic length ℓ_e is needed.

Boundary layers as seen in the discrete dislocation simulations of Shu et al. [28] and the experiments of Sun et al. [29] emerge from the phenomenological nonlocal crystal plasticity theory of Shu and Fleck [13] when the appropriate higher-order boundary conditions are imposed. However, in some cases, reproducing the discrete dislocation behavior

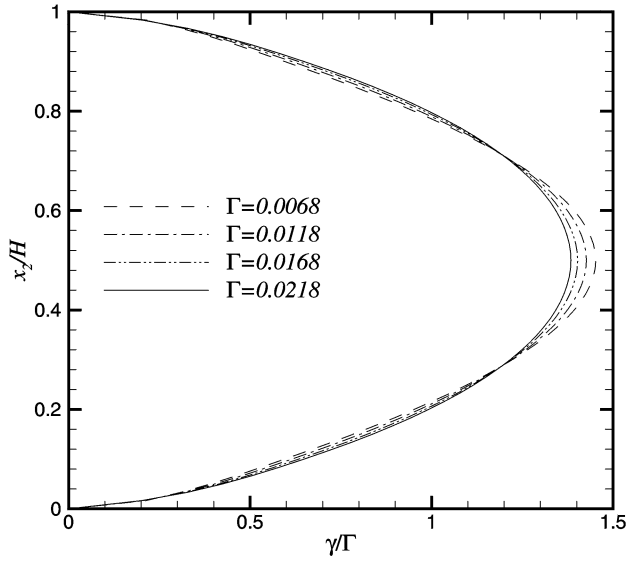

Fig. 11. Shear strain profiles at various values of the overall shear strain Γ predicted by the nonlocal theory for symmetric double slip. From [28].

requires a much larger value of the elastic length scale than seems physically plausible. The comparison with the discrete dislocation results also suggests that the material length scales associated with plastic flow should be taken to evolve with deformation. A framework for specifying the evolution of such material length scales remains to be developed.

5. Concluding remarks

The model composite problem illustrates the important distinction between gradients associated with the density of dislocations that are geometrically necessary and those that are not. The simple shear problem shows the emergence of boundary layers that are precluded by a conventional continuum description of plastic flow. In both problems, there is a distinct size effect that is outside the scope of a conventional plasticity theory.

The discrete dislocation results show size effects in both the hardening and the strength, depending on the particular problem. Phenomenological nonlocal theories have, at least so far, been either strength or hardening based. A hardening-based theory, such as that of Acharya and Bassani [14], uses only ordinary stress measures and boundary conditions and can, in some cases, capture the size-dependent features exhibited by discrete dislocation solutions. However, the existence of boundary layers in simple shear suggest that, in general, a strength-based theory with non-classical stress measures is needed. Each such theory introduces its own type of higher-order boundary condition as well as material properties with the dimensions of length.

At their present stage of development, there are open issues with the details of each of the nonlocal plasticity theories considered. In the theory of Acharya and Bassani [14], how to apportion the incompatibility measure among the various components of the hardening matrix in multiple slip situations is an open issue. In the theory of Shu and Fleck [13], the large value of the elastic length scale needed to obtain predictions consistent with the discrete dislocation results is difficult to justify. Also, in this theory, the fact that the slip gradient measures entering the constitutive relation differ from the corresponding gradients of slip is problematic. The theory of Gurtin [16] is based on the full strain gradient and does not, at least in its present form, distinguish between the components associated with geometrically necessary dislocations and those that are not. Fleck [31] has recently shown that the formulation in [16] can give rise to boundary layer behavior. How predictions based on Gurtin's theory [16] compare with the discrete dislocation simulations remains to be investigated.

The discrete dislocation results also have limitations. The boundary value problems solved in [26–28] are two-dimensional with only edge dislocations. In addition to significantly limiting the types of dislocation interactions, the energy cost of increasing the length of dislocation lines is excluded from the outset. Furthermore, the discrete dislocation formulation is limited to small deformations. There are dislocation structures that emerge at finite strains, under nominally uniform macroscopic deformations (see, e.g., [32]). The theory of Ortiz et al. [17] aims at giving a phenomenological description of such behavior.

The development of a framework for size-dependent plasticity is in a formative stage. The challenge is to derive a phenomenological theory of size-dependent crystal plasticity from the statistical mechanics of discrete dislocations, accounting for geometrically necessary dislocations. Until that happens, comparisons between discrete dislocation plasticity predictions and those of various nonlocal continuum theories can play an important role in identifying the form that a phenomenological size-dependent theory of crystal plasticity should take.

Acknowledgements

Support from the Materials Research Science and Engineering Center on *On Micro- and Nano-mechanics of Materials* at Brown University (NSF Grant DMR-9632524) is gratefully acknowledged.

References

[1] U.F. Kocks, A.S. Argon, M.F. Ashby, Prog. Mater. Sci. 19 (1975) 1.
[2] B. Devincre, L.P. Kubin, Model. Simul. Mater. Sci. Eng. 2 (1994) 559.
[3] B. Devincre, P. Veyssiere, G. Saada, Phil. Mag. A 79 (1998) 1609.
[4] N.A. Fleck, G.M. Muller, M.F. Ashby, J.W. Hutchinson, Acta Metall. Mater. 42 (1994) 475.
[5] K.C. Russell, M.F. Ashby, Acta Metall. 18 (1970) 891.

[6] Q. Ma, D.R. Clarke, J. Mater. Res. 10 (1995) 853.
[7] M.S. De Guzman, G. Neubauer, P. Flinn, W.D. Nix, Mater. Res. Symp. Proc. 308 (1993) 613.
[8] J.S. Stölken, A.G. Evans, Acta Mater. 46 (1998) 5109.
[9] E.C. Aifantis, J. Eng. Mater. Technol. 106 (1984) 326–334.
[10] H.M. Zbib, E.C. Aifantis, Res. Mech. 23 (1988) 261.
[11] R. de Borst, H.-B. Mühlhaus, Int. J. Numer. Meth. Eng. 35 (1992) 521.
[12] N.A. Fleck, J.W. Hutchinson, Adv. Appl. Mech. 33 (1997) 295.
[13] J.Y. Shu, N.A. Fleck, J. Mech. Phys. Solids 47 (1999) 297.
[14] A. Acharya, J.L. Bassani, J. Mech. Phys. Solids 48 (2000) 1565.
[15] Y. Huang, H. Gao, W.D. Nix, J.W. Hutchinson, J. Mech. Phys. Solids 48 (2000) 99.
[16] M. Gurtin, J. Mech. Phys. Solids 48 (2000) 989.
[17] M. Ortiz, E.A. Repetto, L. Stainier, in press.
[18] A. Needleman, Acta Mater. 48 (2000) 105.
[19] I. Groma, P. Balogh, Acta Mater. 47 (1999) 3647.
[20] E. Van der Giessen, A. Needleman, Model. Simul. Mater. Sci. Eng. 3 (1995) 689.
[21] V. Lubarda, J.A. Blume, A. Needleman, Acta Metall. Mater. 41 (1993) 625.
[22] L.P. Kubin, G. Canova, M. Condat, B. Devincre, V. Pontikis, Y. Bréchet, in: G. Martin, L.P. Kubin (Eds.), Nonlinear Phenomena in Materials Science II, Sci-Tech, Vaduz, 1992, p. 455.
[23] D.M. Weygand, L. Friedman, E. Van der Giessen, A. Needleman, Mater. Sci. Eng. A 309–310 (2001) 420.
[24] J.F. Nye, Acta. Metall. 1 (1953) 153.
[25] M.F. Ashby, Phil. Mag. 21 (1970) 399.
[26] H.H.M. Cleveringa, E. Van der Giessen, A. Needleman, Acta Mater. 45 (1997) 3163.
[27] H.H.M. Cleveringa, E. Van der Giessen, A. Needleman, J. Phys. IV 8 (P4) (1998) 83 .
[28] J.Y. Shu, N.A. Fleck, E. Van der Giessen, A. Needleman, in press.
[29] S. Sun, B.L. Adams, W.E. King, Phil. Mag. A 80 (2000) 9.
[30] J.L. Bassani, A. Needleman, E. Van der Giessen, Int. J. Solids Struct., in press.
[31] N.A. Fleck, private communication, 2000.
[32] D.A. Hughes, N. Hansen, Metall. Trans. A 24 (1993) 2021.